Landslide generated tsunamis: A smoking gun in Saratoga Passage, Puget Sound, Washington

William L. N. Whiteaker
Oceanography 499
Senior Thesis
School of Oceanography, University of Washington
w.whiteaker@verizon.net
22 May 2008

Abstract

Landslides, both subaerial and submarine, commonly occur in the Puget Lowland and in Puget Sound. Large coastal landslides can produce tsunamis, thus creating potential hazards in areas that are not in close geographical proximity to the actual landslide. The western coast of Camano Island in northern Puget Sound is characterized by ‘scalloped’ indentations, the largest of which (1500 m x 275 m) is north of Onamac Point; such features are often the result of slope failure. To determine if the Onamac Point morphology was the result of a landslide, a marine geophysical survey and bottom sampling operations were undertaken aboard *R/V Clifford A. Barnes*. Seismic reflection data imaged a large slide mass, consisting of a series of concentric arcuate blocks of deformed glacial sediments, on the bottom of Saratoga Passage in 85 m of water. The volume of material involved in the slide was estimated in two ways. An isopach (thickness) map was prepared using the seismic reflection data, yielding a volume estimate of 17.2×10^6 m^3. Next, the island topography and nearshore bathymetry of the Onamac Point area were used to create a pre-slide or paleosurface. Differencing this surface and the present topography gave a volume of approximately 17.8×10^6 m^3. The offshore slide mass is covered by about 10 m of modern sediments. The average sediment accumulation rate in Puget Sound is about 1.0 cm y^{-1}, suggesting that the Onamac Point landslide occurred about 1000 years ago. This corresponds to the date of a major earthquake in Puget Sound; this M7.5 quake may have triggered the slide. The characteristics of the Onamac Point landslide (volume, slopes, material type) are similar to those of massive tsunamigenic landslides that occurred Alaska in 1958 and in British Colombia in 1975, making the Onamac Point landslide an excellent candidate for tsunami modeling.

Introduction

Puget Sound is a fjord-type estuarine system having unique physiographic and oceanographic characteristics that have been strongly influenced by glacial and tectonic processes. As the Puget Lobe of the Fraser Glaciation retreated, ~15,000 years ago (Downing 1983), glacially carved valleys remained in the Puget Lowland, together with copious amounts of sediment deposited by the retreating glacier. Riverine, lacustrine, and glacio-marine sediments were also deposited rapidly as the glacier retreated (Downing 1983). Erosion and reworking of these glacial features and the overlying sediments has produced what is seen today as a common morphology in the Puget Lowland: deep (200 m), narrow (1-2 km) N-S trending basins bounded by high (90 m), steep (>30º) to vertical bluffs (Figs. 1 and 2).

Tectonic Setting

Seismic events, including ground shaking and faulting, are common in the Puget Lowland (Figs. 2 and 3). This area is a tectonically active and structurally complex zone that is subject to seismic activity from three sources: the subduction zone, the subducting plate itself, and shallow crustal earthquakes (Bucknam et al. 1992). The upper 20 km of crust beneath the Puget Lowland has been deformed into a series of fault-bounded basins and uplifted blocks (Fig. 2) as a result of regional compression caused by northward movement of the Oregon Coast Range block (Pratt et al. 1997). Karlin and Abella (1992) presented evidence for seismic events in the Puget Lowland and slope failure accompanying those events dating back to approximately 3200 ybp, with major seismic events occurring episodically every 200-500 years (Karlin et al. 2004). Evidence for a large seismic event approximately 1000 ybp on the Seattle fault, in the central Puget Lowland, has been presented by Bucknam et al. (1992). This 1000 ybp Seattle fault event has been linked to three simultaneous slope failures by Jacoby et al. (1992). These three slope failures, as large as 500 - 700 m from head scarp to toe, all occurred on the southeastern shore of Mercer Island in Lake Washington. Johnson et al. (2004) published evidence of recurring seismic activity and faulting in the northern Puget Lowland along the Utsalady Point fault (Fig. 2).

Slope Instability

Slope failure occurs when the resisting forces of the slope are overcome by forces acting to move material downslope. Resistive forces include friction and inherent characteristics of the slope material. Some of the forces acting to move material downslope include gravity, water saturation of slope material, slope angle, and ground shaking from seismic events (Keefer 1984, Sylwester and Holmes 1987, Wilson and Keefer 1985). Composition of slope material, especially in regards to porosity, is considered one of the major factors involved in all slope failures (Downing 1983, Keefer 1984, Wilson and Keefer 1985). Slope angle can become over-steepened if material is removed from the foot of the slope by erosive processes. Ground shaking from seismicity can disrupt the resistive forces of friction and material cohesion (Keefer 1984).

Slope failures can pose significant hazards when downslope movement of material results in subaerial deposition (Keefer 1984, Wilson and Keefer 1985). When downslope movement of material results in submarine deposition, a tsunami can be generated, dramatically increasing the hazards associated with slope failure (Hampton et al. 1996, Miller 1960). Slope failure in many of the shoreline bluffs bordering Puget Sound has been shown to result in both subaerial and submarine deposition (Downing 1983, Gonzales et al. 2002).

Landslides in the Puget Lowland

Failure of the slope along bluffs in the Puget Lowland occurs frequently enough to be considered a common hazard (Gonzalez et al. 2002, Karlin et al. 1994) and in some cases slope failure has been catastrophic. Chleborad (1994) details just such a catastrophic landslide which occurred in the Tacoma Narrows region of southern Puget Sound in 1949, involved ~5 x 10^5 m^3 of material, and generated a water wave ~2 m in height.

One of the main factors contributing to landslides in the bluffs bordering Puget Sound is a contact between two separate geologic units within the bluffs, the Esperance Sand and underlying Lawton Clay (Galster and LaPrade 1991). The Esperance Sand layer is more permeable to water, relative to the Lawton Clay, and the plentiful rainfall in the area readily percolates through the sand (Downing 1983). Water does not tend to penetrate the more impermeable clay, but instead builds up in the overlying sand unit. Eventually a critical mass is attained and the slope fails. Landslide scars, where the Esperance Sand and other overlying units have moved downslope exposing the underlying Lawton Clay, are visible in many locations in the Puget Lowland (Downing 1983).

Seismically induced landslides in the Puget Lowland are discussed by Jacoby et al. (1992) and Logan and Walsh (1995). Martin (1995) has also described a landslide located in the central Puget Sound area near Mukilteo which transported a large volume of material, approximately 1.18 x 10^7 m^3, from the nearshore bluffs into the deep waters of Puget Sound. The inferred age of this landslide correlates closely to the time of the event on the Seattle Fault approximately 1000 ybp and may have been triggered by that seismic event. If the landslide wasn't triggered by the seismic event itself, it is possible that the tsunami generated by that event eroded the toe of the bluff, causing the slope to over-steepen and fail (Martin 1995). This landslide transported material in a fluid manner and even though the result was submarine deposition, it probably did not result in a tsunami (Martin 1995).

Seismicity, Landslides, and Tsunamis

Interactions between seismicity, slope failure or landslides, and landslide-generated tsunamis have been studied extensively. Keefer (1984) catalogued forty seismically generated landslides throughout the world. Wilson and Keefer (1985) performed an in depth analysis of seismically generated landslides in California, illustrating the relationship between ground shaking severity and the initiation of different types of slope failure. Hampton et al. (1996) provided an excellent overview of submarine landslides which discusses both the possibility of seismically generated submarine slides and the tsunamigenic potential of such slides.

The first work linking seismicity and tsunamis in Puget Sound was done by Atwater and Moore (1992) and Dinkelman (1993). Both studies correlated the 1000 ybp movement along the Seattle Fault to a tsunami moving northward through Puget Sound. As previously mentioned, Chleborad (1994) analyzed a tsunamigenic landslide with a probable seismic trigger in the Tacoma Narrows region of southern Puget Sound. The landslide occurred on April 16^{th}, 1949, three days after the Puget Sound region experienced a M7.1 earthquake. A 5 cm crack opened, immediately following the earthquake, along the top of the bluff from which the landslide material eventually calved off. The landslide displaced ~5×10^5 m^3 of material and generated a ~2 m tsunami.

Bourgeois and Johnson (2001) have provided additional evidence for tsunamis in Puget Sound and have attempted to determine the ages of the seismic triggers believed responsible for those tsunamis. Gonzalez et al. (2002) provide a summary of the relationships between seismicity, landslides, and tsunamis throughout the Puget Sound region (Fig. 3).

Scope and Objective

The Puget Lowland is densely populated, with extensive industrial and residential developments located upon much of the shoreline of Puget Sound. Slope failure of a shoreline bluff in this region would therefore present a hazard not just for the immediate area, but also throughout the extent of the shoreline any potential tsunami might reach. Understanding the interactions between landslides and potential tsunamis may be a crucial element in mitigating property damage or loss of life throughout the region.

In the northern Puget Lowland, on the western shore of Camano Island, a large cuspate landform was noticed in the regions topography (Figs. 1, 2, and 4). Further examination of this arcuate indentation, which extends landward and northward from Onamac Point, resulted in the hypothesis that this feature was a landslide scar. From the topography, the landslide scar appeared steep, with little to no subaerial deposition visible. Bathymetry data (USCGS 1960) from just offshore of the suspected landslide seemed to suggest the presence of hummocky N-S trending mounds along the bottom of Saratoga Passage.

A marine geophysical expedition was undertaken to map evidence of any submarine deposits resulting from the potential Onamac Point landslide (Fig. 4). Analysis of the collected data would allow a determination to be made as to a) whether the features observed in the topography and bathymetry near Onamac Point represent a landslide scar and subsequent submarine deposition, b) the plausibility of a seismic trigger for the potential landslide, and c) a rough estimate of the tsunamigenic potential of such a landslide.

Independently of these results, this project would add to the growing dataset of information concerning seismicity, landslides, and tsunamis in the Puget Lowland and Puget

Sound. A growing and comprehensive dataset of information may prove pivotal in mitigating the potential hazards associated with these events (Gonzales et al. 2002; Fig. 3).

Methods

A geophysical survey of the suspected Onamac Point landslide area was carried out during a cruise of the *R/V Clifford A. Barnes* in April 2003. Swath bathymetry data was provided courtesy of a subsequent cruise of the *R/V Thomas G. Thompson* in 2004. The data collected during the cruise in April 2003 included a suite of seismic reflection profiles and a piston core (Fig. 4). The seismic reflection data were captured along a series of track lines passing over the suspected depositional mass. Four of the track lines were run parallel to the shoreline. Track line 9 was run perpendicular to the shoreline along the suspected center of the deposition. Two additional track lines, 6 and 7, were run respectively from the northern and southern headlands of the suspected landslide scar, bounding or near bounding the inferred northern and southern extent of the submarine deposition, and converging at the furthest seaward extent of the perpendicular to shore track line (Fig. 4).

Ship speed during collection of the seismic signal data was 3 knots (~5.6 km h^{-1}). Ship position was verified using GPS. Seismic signal data were generated using a Uniboom (EG&G 234) power source and accompanying sparker cage sled (300 joules). Signals were received via a hydrophone streamer. Seismic signal data were amplified and filtered (300 – 900 Hz) using a analog signal processor (Del Norte 501) and then recorded with an analog chart recorder (EPC 3200) using two channels, both set at 100 lines per inch, and recording intervals of 0.5 seconds (0-375 m) for channel A and 0.25 seconds (0-187.5 m) for channel B. Unfiltered seismic signal data were also recorded digitally using a TEAC digital audio tape (DAT) recorder.

A 5-cm-diameter piston corer with a core barrel length of three meters was used to obtain the piston core sample along track line 9 (Fig 4.). Magnetic susceptibility (MgX) measurements were performed on the piston core using a MS2C ring scanner at 2-cm intervals.

A few months after the cruise on *Barnes,* it was learned that the *R/V Thomas G. Thompson* was going to be working in Saratoga Passage conducting physical and biological work for the PRISM (Puget Sound Regional Synthesis Model) program. A request was made that *Thompson* obtain EM300 swath mapping data along two tracks offshore from Onamac Point. The Kongsberg-Simrad EM300 used by *Thompson* operates at 30 kHz and is capable of mapping a swath (width = 4x water depth) of sea floor at speeds of up to 10 knots (18.5 km hr^{-1}). Data from the tracks were processed using MB System and are shown in Figure 4. Because the data were collected within a period of only two hours, no tidal corrections were made.

Results

Morphology

The seismic profile taken along track line 1, west of the suspected depositional mass, shows a smooth morphology and uninterrupted even distribution of sediment in the deep water of Saratoga Passage (Figs. 4 and 5). Evidence for this quiescent depositional environment is also visible both to the north and south of the suspected depositional mass in the seismic profile taken along track line 2 (Figs. 4 and 6), and again to the west of the suspected depositional mass in the seismic profile taken along track line 7 (Figs. 4 and 7). Swath bathymetry (Fig. 4) also shows characteristically smooth sediments to the north, south, and west of the suspected depositional mass.

In dramatic contrast, the suspected depositional mass itself is clearly visible in the swath bathymetry as mounded concentric ridges appearing on the seafloor just westward of Onamac Point (Fig. 4). It is also easily seen in both N-S (Fig. 6) and E-W (Fig. 7) seismic profiles, where it appears as hummocky, mounded deposits disrupting the otherwise smooth morphology. Both the N-S and E-W extent of this submarine deposition is also recorded in seismic profiles (Figs. 6 and 7). Additionally, in both N-S and E-W seismic profiles over the submarine deposition, a coherent internal reflector is visible (Figs. 6 and 7). The seismic stratigraphy of the depositional mass appears quite different above and below this boundary. Beneath the internal reflector the depositional material is seismically transparent. Above the internal reflector, discontinuous, strong, chaotic reflectors are visible.

Study Site Slopes

Seismic reflection profiles generated along track lines 6, 7, and 9 showed submarine slopes extending landward from the base of the depositional mass. The submarine slope seen in the seismic profile recorded along track line 7 is shown in Figure 7. This slope is even more easily discernable in a true scale section of the seismic profile (Fig. 8). The landward extending submarine slopes recorded in all E-W seismic profiles of the depositional mass were calculated to have slope angles at between 16º and 26º. The most northern slope angle was 16º, the most southern slope angle 22º, and the central slope angle 26º.

Volumes

On all seismic profiles where the depositional mass was visible, the depth of the depositional mass was “binned” into 20 m increments, creating four depth bins: 0-20 m, 20-40 m, 40-60 m, and 60-80 m. An isopach (line of constant thickness) map of the depositional mass was generated from these data (Fig. 9). A polar compensating planimeter was then used to calculate the area between each isopach contour. The area of each contour was multiplied by the depth of each "bin" to calculate the volume of material in each "bin". The volume of all "bins" was added together to determine the total volume of the depositional mass. The volume of the submarine depositional mass, calculated by constructing the isopach map from seismic records, was 17.2 x 10^6 m^3 (Fig. 9).

A second isopach map was generated to determine the volume of material that had been removed from both the subaerial and submarine slopes during the suspected landslide. First a paleosurface (pre-slide) map (Fig. 10) was created by projecting bathymetric and topographic contour lines across the arcuate embayment seen in present topography (USGS 1953) and bathymetry (USCGS 1960). Where the projected contours crossed modern isopleths the height difference was calculated. The height difference data were then plotted and used to generate an isopach map of the material involved in the suspected landslide (Fig. 11). A polar compensating planimeter was again used to calculate the area between each isopach contour. The area of each contour was then multiplied by the height difference of each contour interval to give a volume per contour interval. All contour interval volumes were added to yield a total volume of material involved in the suspected landslide. The volume of material suspected to have been involved in slope failure, calculated by constructing the isopach map from the paleosurface map, was 17.8 x 10^6 m^3 (Fig. 11). These two isopach map derived volumes average to 17.5 x 10^6 m^3 of material involved in the suspected Onamac Point landslide.

Age

As per Karlin et al. (2004) and Miller (1999), the piston core sample was analyzed visually for evidence of any turbidite layers or detritus, which would indicate the contact between modern sediment overburden and the material of the suspected depositional mass.

Similarly, MgX (magnetic susceptibility) data from the piston core sample were also analyzed to determine the contact between modern sediment overburden and the suspected depositional material (Karlin et al. 2004, Miller 1999). The depth of sediment obtained in the piston core sample was 166 cm. Neither visual inspection nor MgX analysis of the piston core sample indicated that the piston corer had completely penetrated the modern sediment overburden and sampled the underlying submarine deposit.

Sediment accumulation rates recorded both for similar areas of Puget Sound, and for areas closest to the submarine deposit, indicate approximately 0.5 – 1.0 cm y^{-1} of sedimentation (Carpenter et al. 1985, Lavelle et al. 1986). From these rates and the depth of penetration of the piston core sample, it can be calculated that the core sample represents a time interval of about 160 – 330 years.

Discussion

Onamac Point Landslides

A submarine depositional mass in Saratoga Passage is clearly visible in swath bathymetry and seismic reflection profiles of the area. Swath imagery shows the mass to be composed of at least two concentric ridges trending N-S and convexly curving away from the arcuate embayment north of Onamac Point (Figs. 4 and 9). Seismic reflection profiles show the deposited submarine mass to be hummocky, displaying substantial topography relative to the surrounding sea floor (Figs. 6 and 7). The mass is clearly identifiable in seismic reflection profiles as a distinct unit, displaying none of the characteristics of ‘normal’ deposition seen in the area. The mass appears to have ‘bulldozed’ its way out into the sediments in Saratoga Passage.

More detailed examination of the seismic profiles reveals that the submarine mass is composed of two separate sections, divided by a coherent internal reflector (Figs. 6 and 7). The lower section is nearly seismically transparent, indicating a mass of fine-grained sediment saturated with water. The upper section shows discontinuous, strong, chaotic reflectors, indicating a more consolidated material. The two-layer composition of the deposit suggests that at least two episodes (landslides) of submarine deposition have occurred. Furthermore, the coherent internal reflector indicates that enough time elapsed between the two episodes for a 'sediment surface' to have developed on the first deposit, before the second episode of deposition took place.

In E-W seismic profiles (Fig. 7) the lower layer of the deposit can been seen curving upwards towards the seafloor. Eventually the lower layer becomes expressed on the seafloor and is visible as the farthest seaward extent of the submarine deposit. This seafloor expression of both the upper and lower layer of the deposit is probably also what is seen in the swath bathymetry as the two concentric ridges. The lower layer of the deposit creates the more seaward ridge while the furthest seaward extent of the upper layer of the deposit creates the more landward ridge.

A double landslide event at Onamac Point is hypothesized. The first landslide that occurred primarily involved the submarine slope north of Onamac Point. The highly saturated submarine sediments moved out into Saratoga Passage for some distance and formed the more seaward ridge seen in the swath bathymetry. These saturated submarine sediments also form the seismically transparent lower layer seen in the seismic reflection profiles. Following the first event, after enough time passed so that a sediment layer had developed on the submarine landslide deposit, a subaerial slope failure occurred. The material involved in the subaerial slope failure, being more cohesive, did not flow as far out into Saratoga passage and formed the inner concentric ridge seen in the swath bathymetry. This more cohesive, consolidated material also forms the upper, more chaotic layer seen in the seismic reflection profiles.

Submarine slopes extend upward and eastward from the base of the landslide mass into the arcuate embayment north of Onamac Point. These submarine slopes provide a continuous path down which material could move from bluff to seafloor during slope failure. Such steeply angled slopes, ~16º-26º, have been shown to be prone to slope failure, or provide pathways for material movement downslope, in other locations in the Puget Sound region (Downing 1983).

The estimated volume of material transported downslope during the combined Onamac Point landslides was 17.8 x 10^6 m^3. The estimated volume of material present in the submarine depositional mass is 17.2 x 10^6 m^3. The close correlation between the amounts of material expected to have been involved in the slope failures, and of material present on the seafloor, is another strong indicator that slope failures have taken place at Onamac Point. One possibility to account for the discrepancy between the amounts of material estimated to have been involved in the landslides vs. the amount of material estimated to be in the depositional mass, is that strong tidal currents may have eroded, or at least prevented deposition of, a significant amount of fine grained material.

Age of the Landslide(s)

Unfortunately the piston core sample did not penetrate completely through the modern sediment overburden and into the depositional mass. Because an accurate measurement of sediment depth overlying the depositional mass could not therefore be obtained, it is not possible to accurately determine the time at which either of the slope failures occurred. However, at least 166 cm of sediment have accumulated on the depositional mass since the last slope failure. The fastest known sedimentation rate for the area is 1.0 cm y^{-1} (Lavelle et al. 1986). This information suggests that the slope failure at Onamac Point could have occurred as recently as 166 ybp (1840s). Had the slides occurred this recently, there would surely be eye-witness accounts or at the very least anecdotal evidence of the slides, none of which has been discovered. Because no historical evidence has been discovered, the precise depth of modern sediment overburden is unknown, and the sedimentation rate in the area may be lower than 1.0 cm y^{-1}, the landslides at Onamac Point are probably much older than 166 ybp.

The seismic reflection data can be also be used to infer an age range for the landslides. The thickness of modern sediment in central Saratoga Passage (Line 1, Fig. 5) and over the distal end and flanks of the landslide deposits (Lines 2 and 7, Figs. 6 and 7) averages about 10 m. Applying published accumulation rates (Carpenter et al. 1985; Lavelle et al. 1986) of 0.5-1.0 cm y^{-1} results in an age range of 1000-2000 ybp. Because of the proximity of the Skagit River to the study site, the accumulation rate is probably more toward the 1.0 cm y^{-1} end of the range, suggesting an initial age of the landslide sequence of probably 1000-1200 ybp. The large earthquake along the Seattle fault (Bucknam et al. 1992), and the resulting tsunami (Atwater and Moore 1992; Dinkelman 1993) occurred within this age range. It is interesting to speculate on the possibility that these two events were related to the Onamac Point landslides and that they were possibly the initiators of the slope failures.

Tsunamigenic Potential

Using Murty's (1979) method for determining the amplitude of a simple solitary water wave generated by a submarine landslide, and abiding by the assumptions he made in completing his calculations, a rough estimate of the height of a tsunami generated by the suspected Onamac

Point landslide was calculated. The equation used in estimating the height of the potential tsunami generated by the suspected Onamac Point landside was:

$$H = 1/D\,[8(3)^{1/2}\mu l h\,(\delta-1)(D-D_s)]^{2/3}$$ (Murty 1979)

where:

H = estimated height of tsunami

D = depth from sea surface to center of landslide mass: after slope failure

D_s= depth from sea surface to center of landslide mass: prior to slope failure

μ = 0.01 from Murty (1979)

l = length of landslide mass perpendicular to shoreline: prior to slope failure

h = thickness of landslide mass: prior to slope failure

δ = 2 from Murty (1979)

A paleosurface profile perpendicular to the shoreline and centered in the arcuate embayment north of Onamac Point was prepared and used to calculate *l*, *h*, and D_s. D was calculated from seismic reflection profiles recorded over the submarine deposit (Figs. 6 and 7). The equation and assumptions provided by Murty (1979), coupled with the parameters specific to Onamac Point, yields the following:

$$H = 1/D\,[8(3)^{1/2}\mu l h\,(\delta-1)(D-D_s)]^{2/3}$$

where:

H = estimated height of tsunami

D = 85 m

D_s= 20 m

μ = 0.01 from Murty (1979)

l = 400-500 meters

h = 15 m

δ = 2 from Murty (1979)

Completing the calculation using the parameters specific to Onamac Point suggests that the submarine portion of the suspected Onamac Point landslide produced a tsunami that may have exceeded 15 m to 17 m in height.

The equation used in estimating tsunami height from submarine landslides has been shown to overestimate the resulting tsunami by ~20% (Murty 1979). Taking that into account, the possible tsunami height resulting from the submarine Onamac Point landslide is still in the range of 12-13 m.

An additional consideration specific to the suspected Onamac Point landslide must be taken into account. Murty's (1979) calculations were used to determine tsunami height generated by a wholly submarine landslide. The suspected Onamac Point landslide included a subaerial component whose impact on tsunami generation could be not estimated using Murty's (1979) methods. Due to the complexities involved in calculating the tsunamigenic potential of subaerial landslides, performing such a calculation for the subaerial Onamac Point landslide was beyond the scope of this project. Therefore the tsunamigenic potential of the subaerial Onamac Point landslide has been ignored. However, it seems doubtful that with the amount of material involved, the steepness of the slope down which the material moved, and the depth of water into which the material moved, that the sea surface would not have been disturbed by the subaerial Onamac Point landslide.

Because of the highly generalized assumptions used in the preceding calculation, and the inability to integrate any subaerial component of the suspected landslide, the preceding calculation can only be considered a very rough estimate of any tsunamigenic potential.

Comparison of Tsunamigenic Potential

Table 1 presents characteristics of landslides that have similar regional settings to the Onamac Point landslides and are known to have been tsunamigenic. The previously discussed Tacoma Narrows landslide was explicitly detailed by Chleborad (1994). The Tacoma Narrows landslide occurred in the south Puget Sound region in 1949 and from eyewitness accounts generated a tsunami ~2.5 m in height (Chleborad 1994). The Lituya Bay landslide followed an earthquake in Alaska in 1958 and occurred in a steep walled, deep water, fjord type setting (Miller 1960). The Lituya Bay landslide generated one of the largest water waves ever recorded, a mega tsunami with water run-up of ~500m (Miller 1960). The Kitimat Inlet submarine landslide occurred in British Colombia in 1975 and generated a tsunami ~4.6 m in height (Murty 1979).

The similarities in physical characteristics between the Onamac Point landslides and known tsunamigenic landslides are striking (Table 1). The material involved in the Onamac Point slides appears to have been moved as fairly stable units, or “blocks”, just as with the known tsunamigenic slides. Both the known tsunamigenic slides and the Onamac Point slides transported large volumes of material. In all cases landslide material was transported down steep slopes and into deep water. Velocities for the Onamac Point landslides were averaged from other known tsunamigenic landslides. The similar characteristics to known tsunamigenic landslides, calculated tsunamigenic potential, and sheer volume of material involved in the Onamac Point landslides, pose a significant argument for the Onamac Point landslides to have generated tsunamis up to 13 m high in Saratoga Passage.

Conclusions

Obvious submarine deposition due to two massive landslides has occurred at the base of the arcuate embayment that trends northward from Onamac Point. The deposited material is highly visible in seismic reflection and swath map records of the area. The material appears to be divided into two sections, with a lower less consolidated layer up to 40 m thick overlain by an upper more consolidated layer about 35 m thick . The lower layer extends farther out into Saratoga Passage than the upper layer. This suggests that slope failure occurred in two stages: first a submarine landslide, then a subaerial landslide. A coherent internal reflector visible in the seismic profiles indicates that some time elapsed between the two events.

Steep submarine slopes in the area extend from the base of the submarine deposition up into the embayment, suggesting a possible path on which downslope movement of material occurred. The amount of material estimated to have moved downslope (17.8×10^6 m^3) correlates closely with the amount of material in the submarine deposit (17.2×10^6 m^3). The age of the submarine deposit could not be determined, but seismic reflection data and published sediment accumulation data suggest that the landslides occurred 1000-1200 ybp. The submarine Onamac Point landslide by itself had the potential to generate a tsunami 12-13 m in height. From comparisons with other similar landslides, it seems highly unlikely that the subaerial portion of the Onamac Point landslide would not also have generated a tsunami.

Future Work

Obtaining a complete swath bathymetry map of the landslide deposit would be helpful in visualizing the morphological details of the landslide. Such a map might also unlock further clues as to how the slide progressed and the nature of the slide deposit itself.

Piston core samples of both the underlying layer and overlying layer of the deposit would help in determining material composition. Such information could be used to correlate deposit material with material in the bluff bounding the subaerial arcuate embayment, possibly yielding a better understanding of how and why the bluff failed. Sediment overburden from deeper piston cores could also be used to accurately determine the age of the landslides, perhaps allowing correlation of the slope failures to known seismic events.

Just 5-6 km west of Onamac Point, on the steep eastern shore of Whidbey Island, are two low spits that shelter Race and Harrington Lagoons. It is entirely possible that run-up from a tsunami generated by the Onamac Point landslide(s) could have deposited sand sheets in these low areas. Such deposits would probably be at a depth of 1-2 m or less and could be recovered using standard soil boring equipment. Recovery of such samples would also permit dating the tsunamigenic event.

A comprehensive model of the potential tsunamis resulting from the Onamac Point landslides would be of enormous benefit. This benefit would extend beyond just the inherent knowledge gained by such a model. Such information could assist in educating the general public to the hazards posed by tsunamis in Puget Sound and aid policy makers in mitigating those hazards. If such tsunamis have happened previously, it is entirely plausible that they will happen again.

Acknowledgements

This project was completed in two separate legs, spanning five years, and changed dramatically during that process. I would like to thank Hal Mofjeld and Vasily Titov for their time and assistance with the origination of this project in 2003. I would like to thank Jill Coyle and the crew of the *R/V Clifford A. Barnes* for all the help during the 2003 cruise. I would also like to thank Miles Logsdon for his help with trying to get all the data sorted out way back in 2003. Last but most certainly not least, I would like to thank Mark Holmes for his continued patience, perseverance, and enormous assistance in completing this project, both in 2003 and in 2008. Without your help and guidance, not to mention allowing me to return and finish, this project would have never been completed. I thank you Mark.

References

Atwater, B., and A. Moore. 1992. A tsunami about 1000 years ago in Puget Sound, Washington. Science **258**: 1614-1617.

Bourgeois, J., and S. Y. Johnson. 2001. Geologic evidence of earthquakes at the Snohomish delta, Washington, in the past 1200 years. Geo. Soc. Amer. Bull. **113**: 482-494.

Bucknam, R. C., E. Hemphill-Haley, and E. B. Leopold. 1992. Abrupt uplift within the past 1700 years at southern Puget Sound, Washington. Science **258**: 1611-1614.

Carpenter, R., M. L. Peterson, and J. T. Bennett. 1985. ^{210}Pb-Derived sediment accumulation and mixing rates for the greater Puget Sound region. Marine Geology **64**: 291-312.

Chleborad, A. F. 1994. Modeling and analysis of the 1949 Narrows Landslide, Tacoma, Washington. Bull. Assoc. Eng. Geologists **3**: 305-327.

Dinkelman, L. 1993. Wave height estimation of a tsunami in Puget Sound. Unpublished thesis, University of Washington.

Downing, J. 1983. The coast of Puget Sound – Its processes and development. Puget Sound Books, Washington Sea Grant/University of Washington Press.

Finlayson, D. P., R. A. Haugerud, and H. R. Greenberg. 2001. Building a seamless digital elevation model of the Puget Sound basin, Puget Sound regional research 2001: Abstracts & biographies, Puget Sound Water Quality Action Team, Olympia, WA.

Galster, R. W. and W. T. Parade. 1991. Geology of Seattle. Bull. Assoc. Eng. Geologists **28**: 267-302.

González, F., B. Sherrod, B. Atwater, A. Frankel, S. Palmer, M. Holmes, B. Karlin, B. Jaffe, V. Titov, H. Mofjeld, and A. Venturato. 2002. A Contribution to the inundation mapping project of the U.S. national tsunami hazard mitigation program. Unpublished workshop report, National Oceanic and Atmospheric Administration.

Hagstrum, J.T., D.A. Swanson, and R.C. Evarts. 1998. Paleomagnetism of an east-west transect across the Cascade are in southern Washington: Implications for regional tectonism. J. Geophys. Res. **104**: 12,853.

Hampton, M. A., H. J. Lee, and J. Locat. 1996. Submarine landslides. Rev. Geophys. **34**: 33 59.

Jacoby, G. C., P. L. Williams, and B. M. Buckley. 1992. Tree ring correlation between prehistoric landslides and abrupt tectonic events in Seattle, Washington. Science **258**: 1620-1623.

Johnson, S.Y., C.J. Potter, and J.M. Armentrout. 1994. Origin and evolution of the Seattle fault and Seattle basin, Washington. Geology **22**: 71-74.

Johnson, S.Y., C.J Potter, J.M Armentrout, J.J. Miller, C.A. Finn, and C.S. Weaver. 1996. The southern Whidbey Island Fault; an active structure in the Puget Lowland, Washington: Geological Society of America Bulletin **108**: 334-354.

Johnson, S.Y., A.R. Nelson, S.F. Personius, R.E. Wells, H.M. Kelsey, B.L. Sherrod, K. Okumura, R. Koehler III, R.C. Witter, L-A. Bradley, and D.J. Harding. 2004. Evidence for late Holocene earthquakes on the Utsalady Point fault, northern Puget Lowland, Washington. Bull. Seis. Soc. Amer. **94**: 2299-2316.

Karlin, R. E., and S. E. B. Abella. 1992. Paleoearthquakes in the Puget Sound region recorded in sediments from Lake Washington, U.S.A. Science **258**: 1617-1620.

Karlin, R. E., M. L. Holmes, and S. E. B. Abella. 1994. Holocene neotectonic deformation and earthquake history in sediments from Lake Washington. Abstracts with Program, Geol. Soc. Amer. **26**: 522.

Karlin, R. E., M.L. Holmes, S.E.B. Abella, and R.E. Sylwester. 2004. Holocene landslides and a 3500-year record of Pacific Northwest earthquakes from sediments in lake Washington. Geol. Soc. Amer. Bull. **116**: 94-108.

Keefer, D. K. 1984. Landslides caused by earthquakes. Geo. Soc. Amer. Bull. **95**: 406-421.

Lavelle, J. W., G. J. Massoth, and E. A. Crecelius. 1986. Accumulation rates of recent sediments in Puget Sound, Washington. Marine Geology **72**: 59-70.

Logan, R. L., and T. J. Walsh. 1995. Evidence for a large prehistoric seismically induced landslide into Lake Sammamish. Washington Geology **23**: 3-5.

Martin, A. 1995. Submarine and subaerial landslides as mechanisms of large-scale sediment transport into a deep-water estuary, Puget Sound, Washington. School of Oceanography, University of Washington. Unpublished Manuscript.

Miller, D. J. 1960. Giant waves in Lituya Bay Alaska. U.S.G.S. Professional Paper 354-C.

Miller, L. C. 1999. Landslide occurrence and frequency in Puget Sound, Washington; magnetic susceptibility analysis of piston core samples collected between Edmonds and Mukilteo. School of Oceanography, University of Washington. Unpublished Manuscript.

Murty, T. S. 1979. Submarine slide-generated water waves in Kitimat Inlet, British Colombia. J. Geophys. Res. **84**: 7777-7779.

Nixon, R. 1994. Tsunamigenic deposits in Puget Sound: Implications for paleoseismicity. Unpublished thesis, University of Washington.

Pratt, T.L, C. Potter, W. Stephenson, and C. Finn. 1997. Seismic reflection images beneath Puget Sound: The Puget Lowland thrust sheet hypothesis. J. Geophys. Res. **102**: 27,469-489.

Sherrod, B. L., T. M. Brocher, C.S. Weaver, R. C. Bucknam, R. J. Blakely, H. M. Kelsey, A. R. Nelson and R. Haugerud. 2004. Holocene fault scarps near Tacoma, Washington, USA, Geology **32**: 9-12.

Sylwester, R. E., and M. L. Holmes. 1987. Marine geophysical evidence of a recent submarine slope failure in Puget Sound Washington. Proceedings, Oceans 89 **5:** 1524-1529.

U.S. Coast and Geodetic Survey. 1960. Bathymetric Survey H-8544.

U.S. Geological Survey. 1953. Camano, Washington 7 ½ Min. Quadrangle. N4807.5-W12230/7.5

Wilson, R. C., and D. K. Keefer. 1985. Predicting areal limits of earthquake-induced landsliding, p. 317-345, 492-494, *In* J. I. Ziony [ed.], Evaluating earthquake hazards in the Los Angeles region, U.S.G.S. Professional Paper 1360.

Table 1. Parameters of some large submarine and subaerial tsunamigenic landslides compared to those of the Saratoga Passage (Onamac Point) landslide.

Location	**Kitimat Inlet** (Murty 1979)	**Lituya Bay** (Miller 1960)	**Tacoma Narrows** (Chleborad 1994)	**Saratoga Passage (Onamac Point)**
Type	Horizontal block	Vertical block	Vertical block	**Vertical and Horizontal blocks**
Size	27×10^6 m^3	40×10^6 m^3	5×10^5 m^3	**17.5×10^6 m^3**
Slope	8^o	40^o	$15\text{-}35^o$	**$16\text{-}26^o$**
Water Depth	90 m	120 m	50 m	**85 m**
Velocity	86 km h^{-1}	60 km h^{-1}	40 km h^{-1}	**~50 km h^{-1}**
Tsunami Height	4.3-8.2 m	30-150 m	2.5 m	**~13 m**

Figure Captions

Figure 1. Physio-topographic map of northern Puget Sound showing locations of Saratoga Passage, Camano Island, and the study site at Onamac Point. Whidbey Island and Livingston Bay are labeled for geographic reference. Inset: Regional scale physio-topographic map of Puget Sound showing location of study site. Modified from Finlayson et al. 2001.

Figure 2. Map of Puget Lowland showing study site on the west side of Camano Island. Dashed lines indicate locations of major fault zones: UPF – Utsalady Point Fault (Johnson et al. 2004), SWIF – Southern Whidbey Island Fault (Johnson et al. 1996), HCF – Hood Canal Fault (Pratt et al. 1997), SF – Seattle Fault (Johnson et al. 1994), PF – Puget Fault (Johnson et al. 1994), TCBF – Tacoma-Commencement Bay Fault (Sherrod et al. 2004), and SHF – Saint Helens Fault (Hagstrum et al. 1998). Circled T's indicate tsunami deposits resulting from the 1000 ybp event along the Seattle Fault: Livingston Bay (Nixon 1994), the Snohomish River Delta (Bourgeois and Johnson 2001), Cultus Bay (Atwater and Moore 1992), and West Point (Atwater and Moore 1992).

Figure 3. Tsunami hazard map of Puget Sound showing possible tsunami source zones and regional evidence for past tsunamis. The high priority tsunami source zone area of northern Puget Sound encompasses the study site and nearby waters. Steep topography bounding deep water is indicated for the study site. Locations of major fault zones are shown by dashed lines. Modified from Gonzales et al. 2002.

Figure 4. Map of study area displaying tracks (thin black lines) of the geophysical survey and the location of the piston core sample. Locations of seismic reflection sections described in text along track Line 1 (Fig. 5), Line 2 (Fig. 6), and Line 7 (Fig. 7) are in bold. Two concentric ridges curving convexly away from the arcuate embayment north of Onamac point are visible in the swath bathymetry of the submarine depositional mass. Steep bluffs bounding the embayment are discernable in the topography (USGS 1953).

Figure 5. Seismic reflection profile recorded along track line 1 (Fig. 4) showing "normal" smooth sea floor morphology and post-glacial sediment section beneath central Saratoga Passage. Vertical exaggeration x5.

Figure 6. Seismic reflection profile recorded along track line 2 (Fig. 4) showing the N-S extent of the submarine depositional mass. Vertical exaggeration x5. The morphology of the mass appears as hummocky mounds relative to the "normal" smooth seafloor morphology seen both to the north and south of the depositional mass. Base of the depositional mass is shown by red dots. A coherent internal reflector divides the mass approximately in half. Below the internal reflector the mass is nearly seismically transparent, indicating a fine-grained water saturated deposit. Above the reflector a much stronger seismic signal returned, indicating the upper layer is composed of much more cohesive material.

Figure 7. An E-W seismic reflection profile recorded along track line 7 near the mid-southern portion of the depositional mass (Fig. 4). Vertical exaggeration x5. The morphology of the depositional mass appears as hummocky mounds relative to the smooth seafloor morphology

seen to the west of the depositional mass. The base of the depositional mass is shown by red dots. A steep submarine slope extending from the base of the mass upward and eastward into the embayment north of Onamac Point (Fig. 4) is visible on the right side of the image. A coherent internal reflector divides the mass approximately in half. Again, seismically transparent or near transparent deposits can be seen to compose the lower portion of the mass, with stronger seismic signal return seen from the material deposited above the reflector. The lower layer can be seen curving upward to the seafloor and extending farther seaward than the upper layer.

Figure 8. Diagram of the depositional mass as derived from the seismic reflection profile taken along track line 7 (Figs. 4 and 7). Diagram is true 1:1 scale and shows the E-W extent and depth of the depositional mass. Base of the depositional mass is in red while the current seafloor is in blue. The hummocky morphology of the mass in comparison to the smoother seafloor seen to the west of the mass is evident. The steep submarine slopes extending upward and eastward of the depositional mass are also evident.

Figure 9. Isopach map of the submarine depositional mass, as derived from seismic reflection profiles of the area, shown by red concentric lines (20 m interval). Black lines indicate tracks along which the seismic reflection profiles were recorded (Fig. 4). Two concentric ridges curving away from the arcuate embayment north of Onamac Point are visible in the swath bathymetry. The isopach map of the submarine depositional material and the ridges seen in the swath imagery show strong correlation. The volume of material in the submarine depositional mass was calculated to be 17.2×10^6 m^3.

Figure 10. Modern topography (USGS 1953) and bathymetry (USCGS 1960) are shown in black (10 m contour interval). The paleosurface, or pre-slide surface, is shown in red. The "seam" between topography and bathymetry is the contour of zero elevation, shown in bold black and bold red respectively.

Figure 11. Red lines form an isopach map (10 m contour interval), derived from the paleosurface map (Fig. 10), of the material involved in the suspected slope failure. Present day topography (USGS 1953) and bathymetry (USCGS 1960) are shown in black (10 m contour interval). Volume of material involved in the suspected slope failure was calculated to be 17.8 x 10^6 m^3.

Figure 1

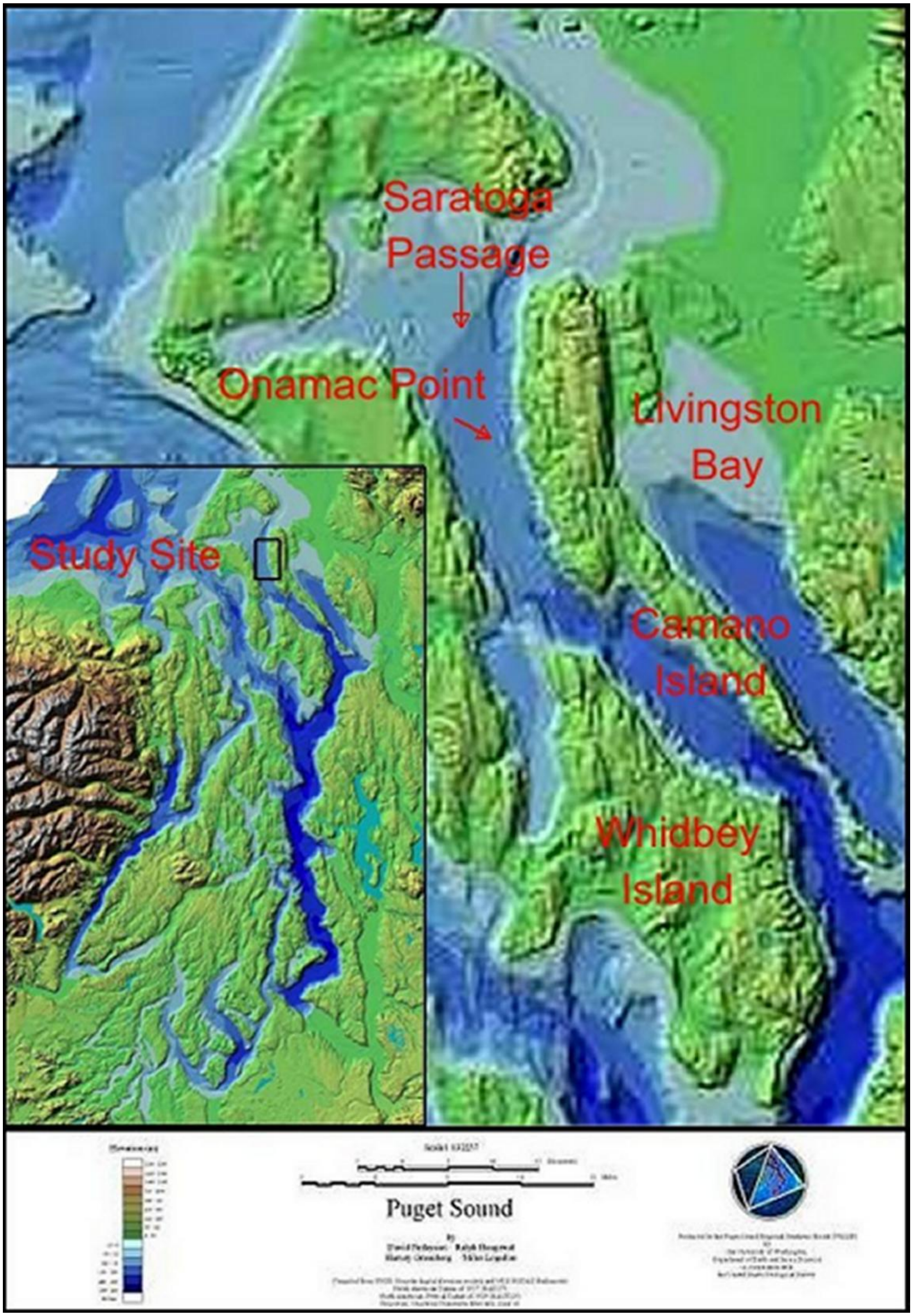
Saratoga
Passage
Onamac Point
Livingston
Bay
Study Site
Camano
Island
Whidbey
Island
Puget Sound

Figure 2

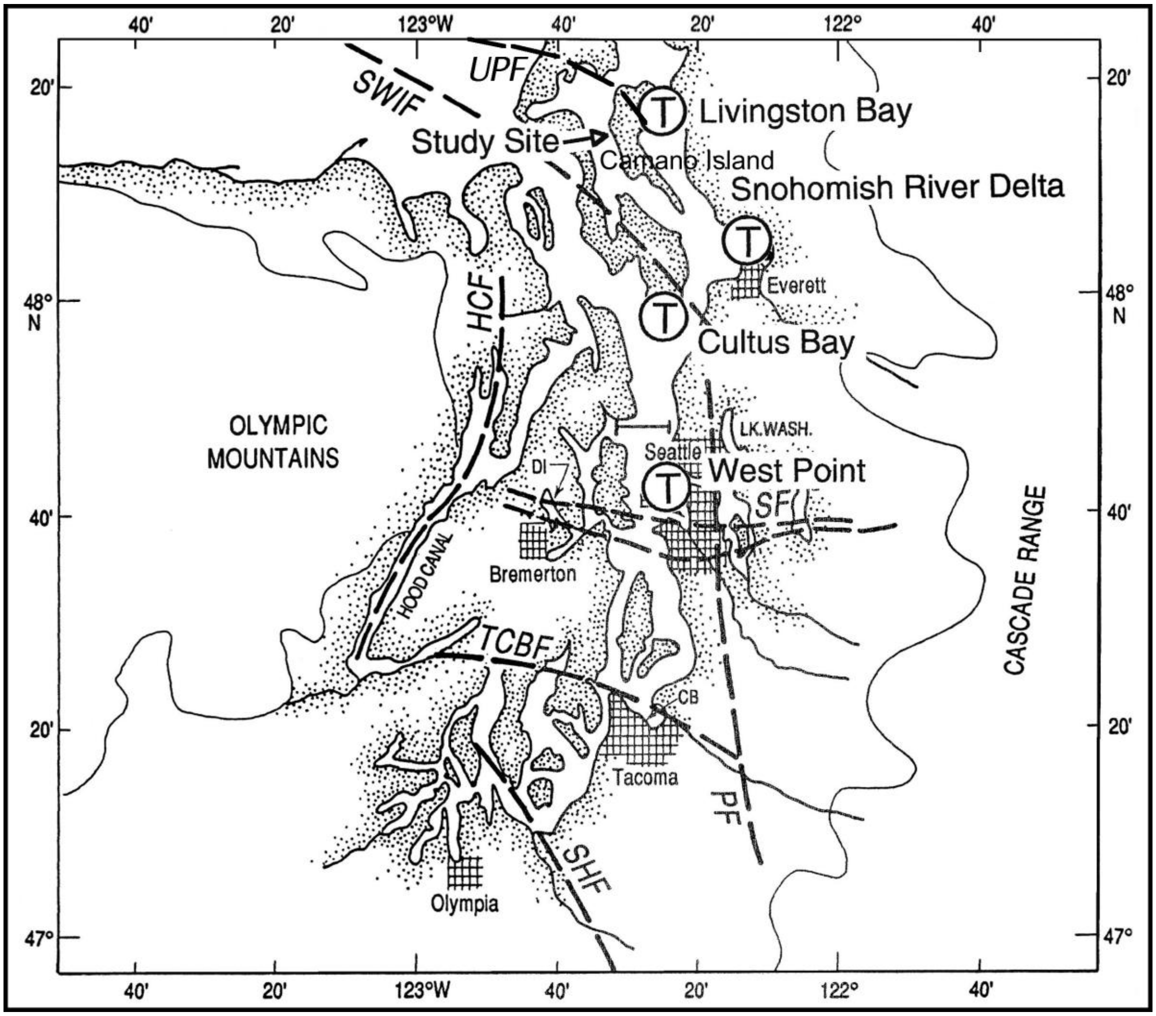
40'
20'
123°W
40'
20'
122°
40'
20'
48°
N
40'
20'
47°
SWIF
UPF
Study Site
Livingston Bay
Camano Island
Snohomish River Delta
Everett
Cultus Bay
HCF
OLYMPIC
MOUNTAINS
LK.WASH.
Seattle
West Point
DI
SF
Bremerton
HOOD CANAL
TCBF
CB
Tacoma
PF
SHF
Olympia
CASCADE RANGE

Figure 3

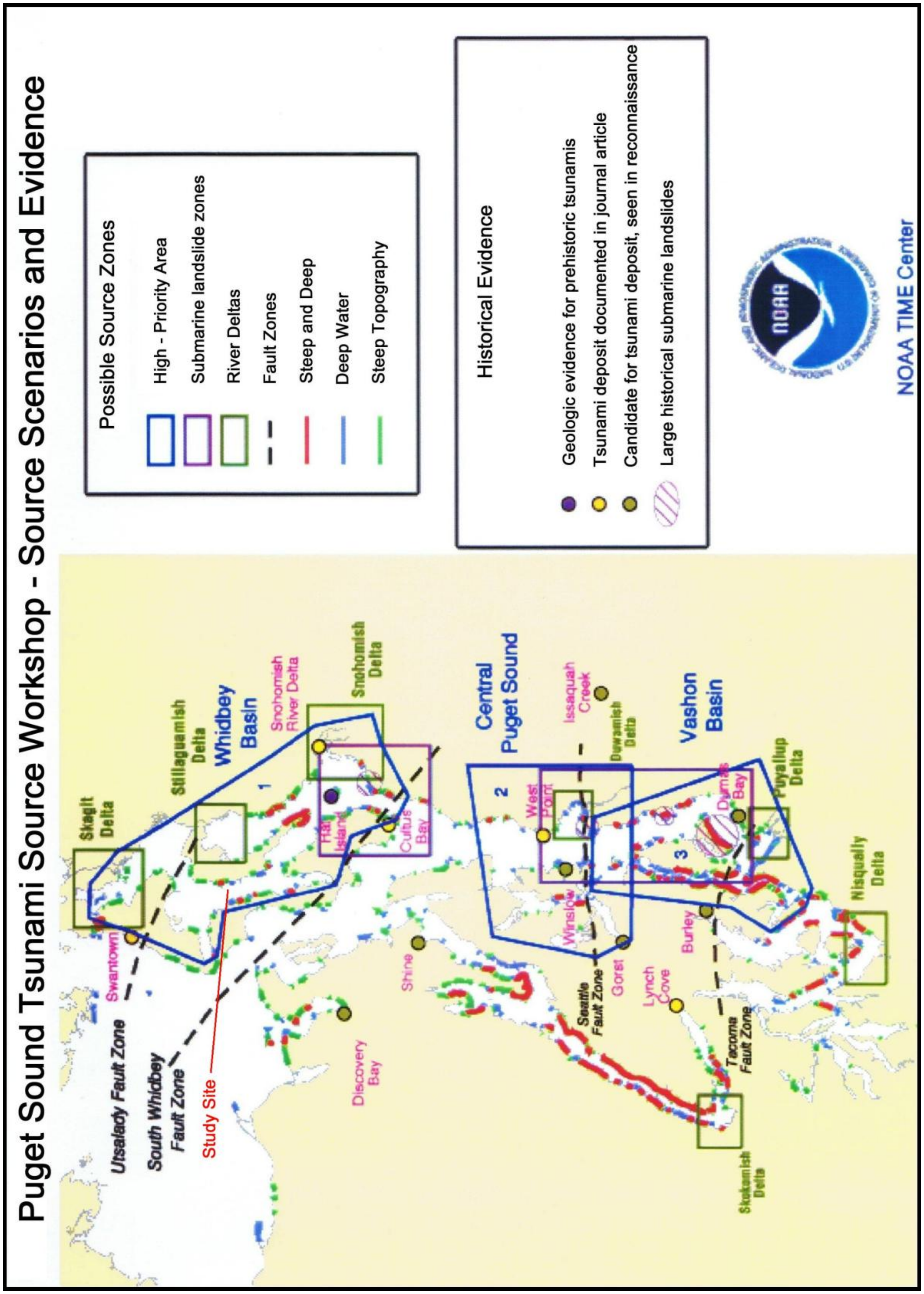

Puget Sound Tsunami Source Workshop - Source Scenarios and Evidence
Possible Source Zones
High - Priority Area
Submarine landslide zones
River Deltas
Fault Zones
Steep and Deep
Deep Water
Steep Topography
Historical Evidence
Geologic evidence for prehistoric tsunamis
Tsunami deposit documented in journal article
Candidate for tsunami deposit, seen in reconnaissance
Large historical submarine landslides
NOAA TIME Center
Utsalady Fault Zone
South Whidbey Fault Zone
Study Site
Swantown
Skagit Delta
Stillaguamish Delta
Whidbey Basin
Snohomish River Delta
Snohomish Delta
Cultus Bay
Discovery Bay
Shine
Central Puget Sound
Issaquah Creek
Duwamish Delta
West Point
Winslow
Seattle Fault Zone
Gorst
Lynch Cove
Burley
Vashon Basin
Dumas Bay
Puyallup Delta
Nisqually Delta
Tacoma Fault Zone
Skokomish Delta
1
2
3

Figure 4

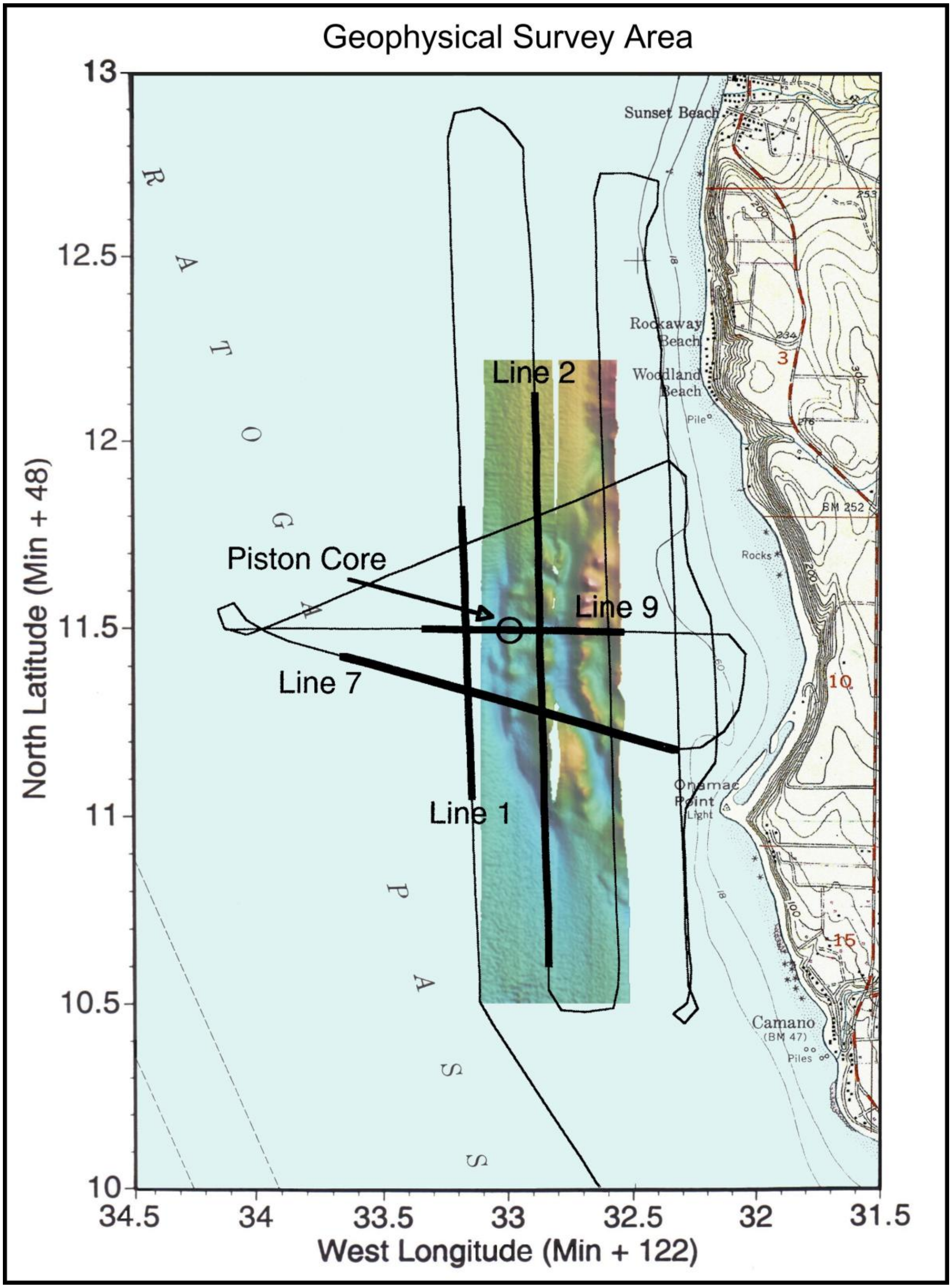
Geophysical Survey Area
North Latitude (Min + 48)
West Longitude (Min + 122)
13
12.5
12
11.5
11
10.5
10
34.5
34
33.5
33
32.5
32
31.5
Line 2
Line 9
Line 7
Line 1
Piston Core
Sunset Beach
Rockaway Beach
Woodland Beach
Onamac Point Light
Camano
Rocks
Pile
Piles
BM 252
(BM 47)
R A T O G A P A S S

Figure 5

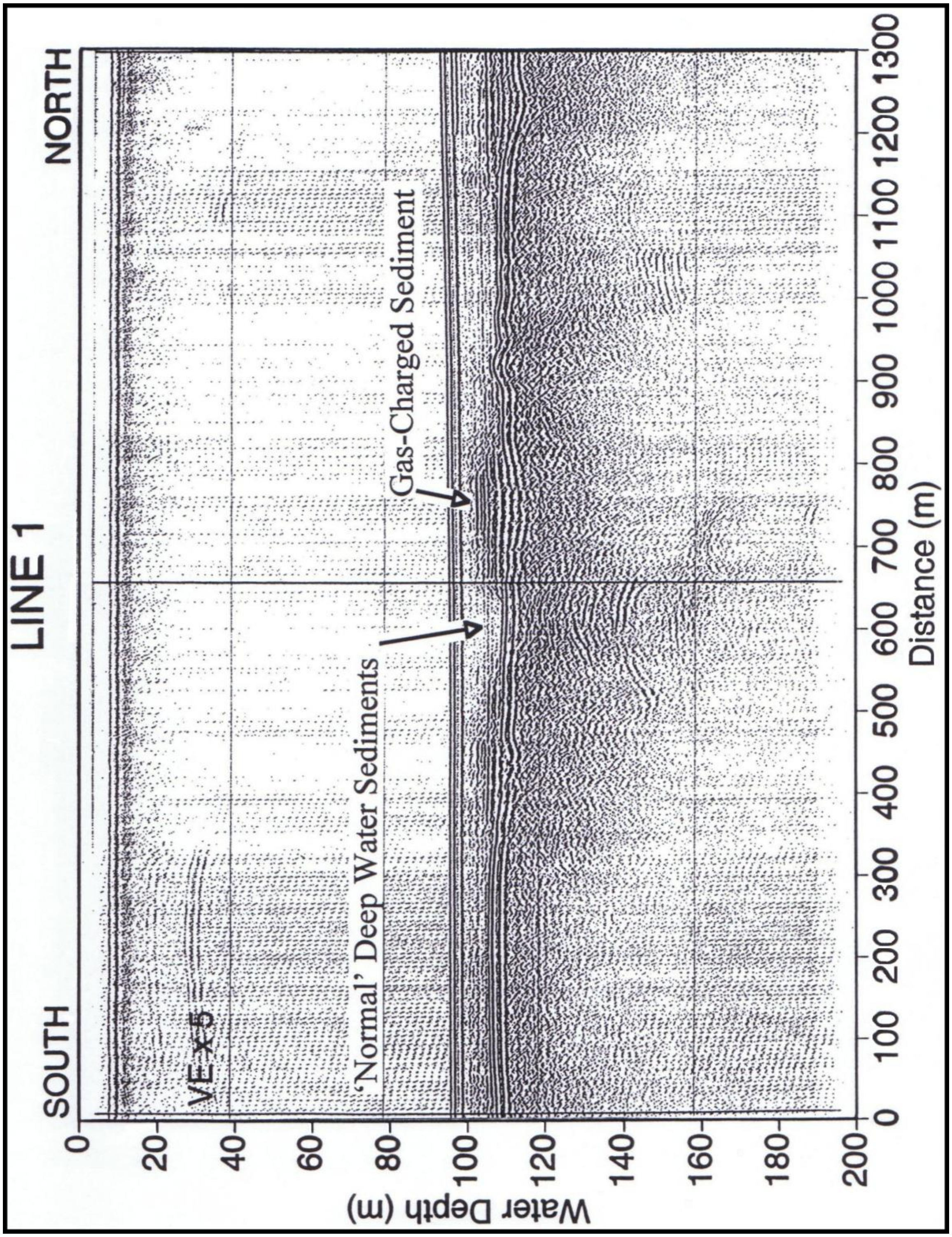
LINE 1
SOUTH
NORTH
VE x 5
'Normal' Deep Water Sediments
Gas-Charged Sediment
Distance (m)
Water Depth (m)

Figure 6

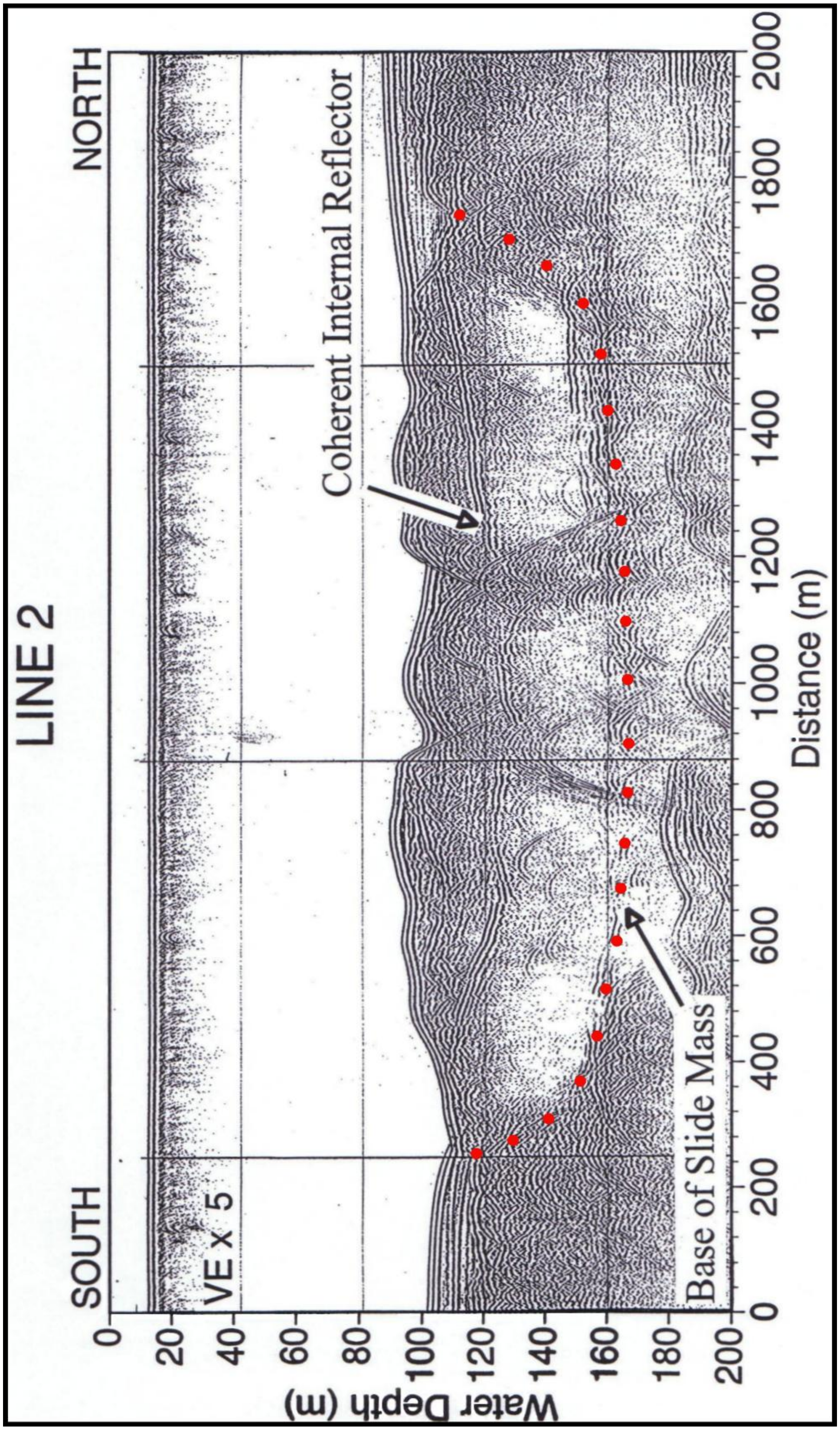
LINE 2
SOUTH
NORTH
VE x 5
Coherent Internal Reflector
Base of Slide Mass
Distance (m)
0
200
400
600
800
1000
1200
1400
1600
1800
2000
Water Depth (m)
0
20
40
60
80
100
120
140
160
180
200

Figure 7

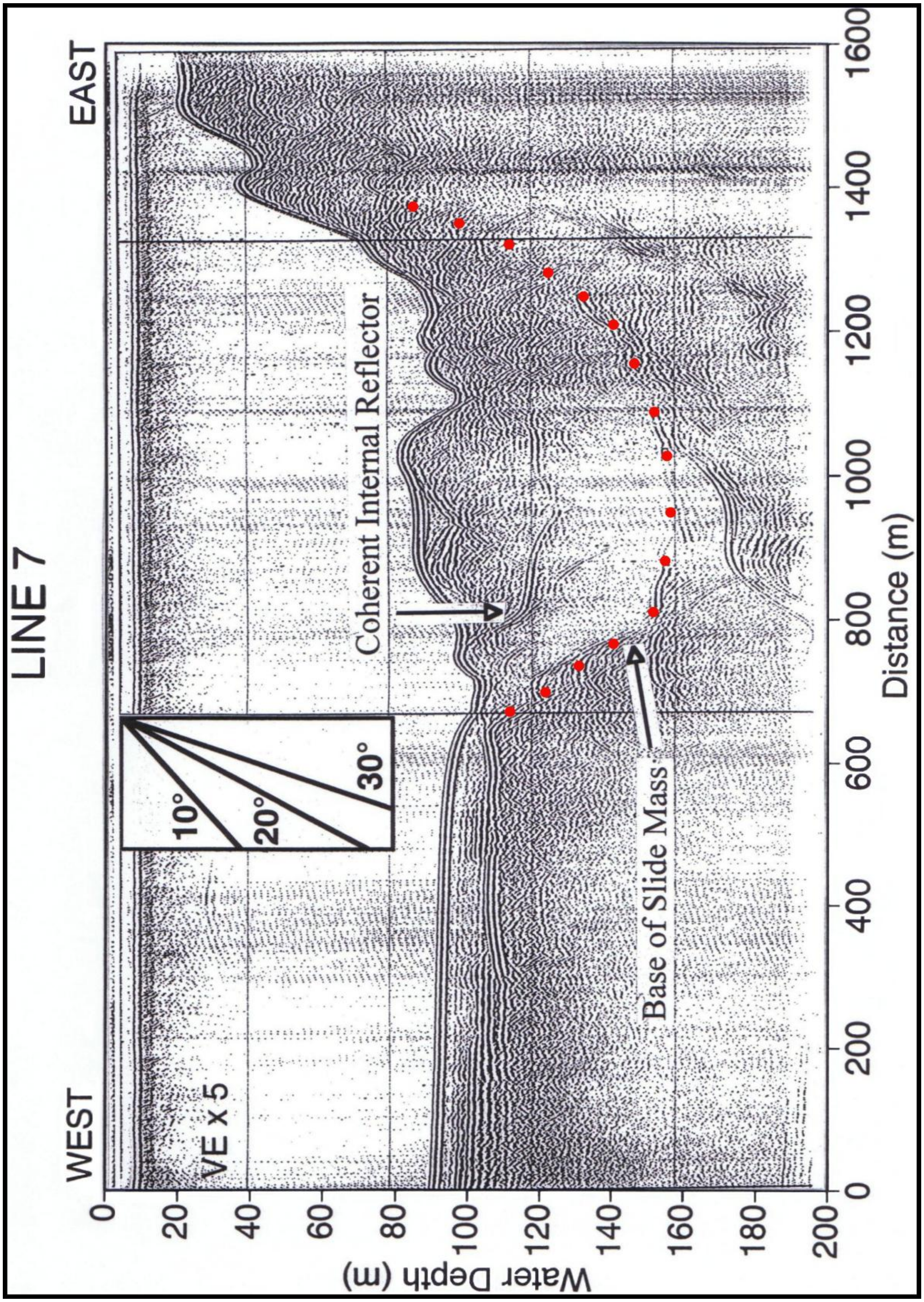

LINE 7
WEST
EAST
VE x 5
10°
20°
30°
Coherent Internal Reflector
Base of Slide Mass
Water Depth (m)
Distance (m)
0
20
40
60
80
100
120
140
160
180
200
0
200
400
600
800
1000
1200
1400
1600

Figure 8

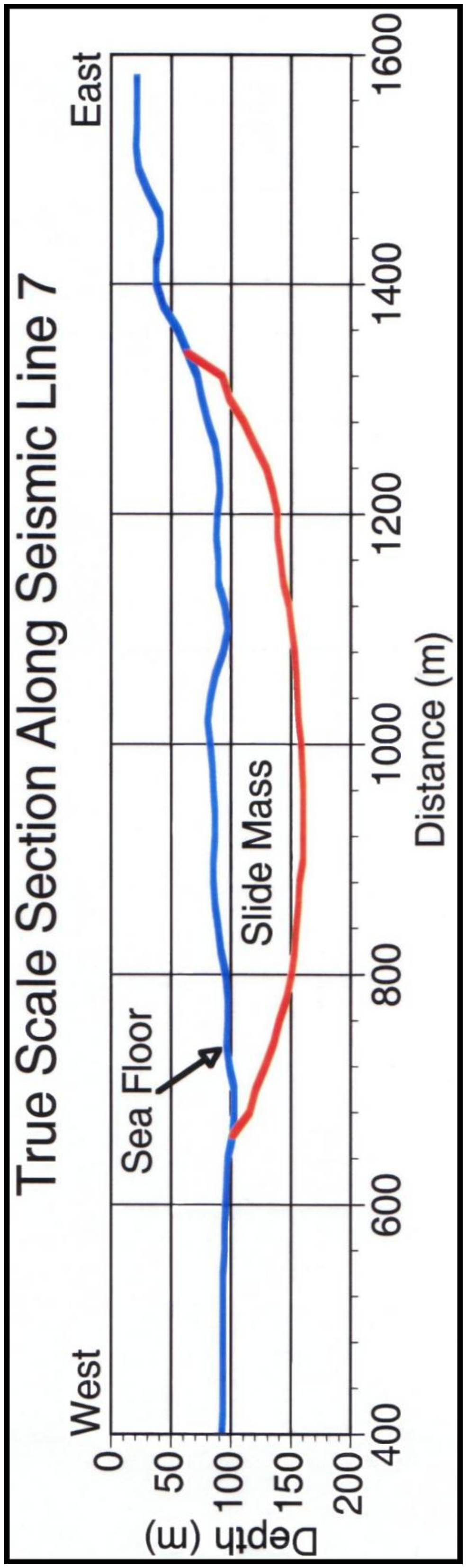
True Scale Section Along Seismic Line 7
West
East
Sea Floor
Slide Mass
Depth (m)
0
50
100
150
200
400
600
800
1000
1200
1400
1600
Distance (m)

Figure 9

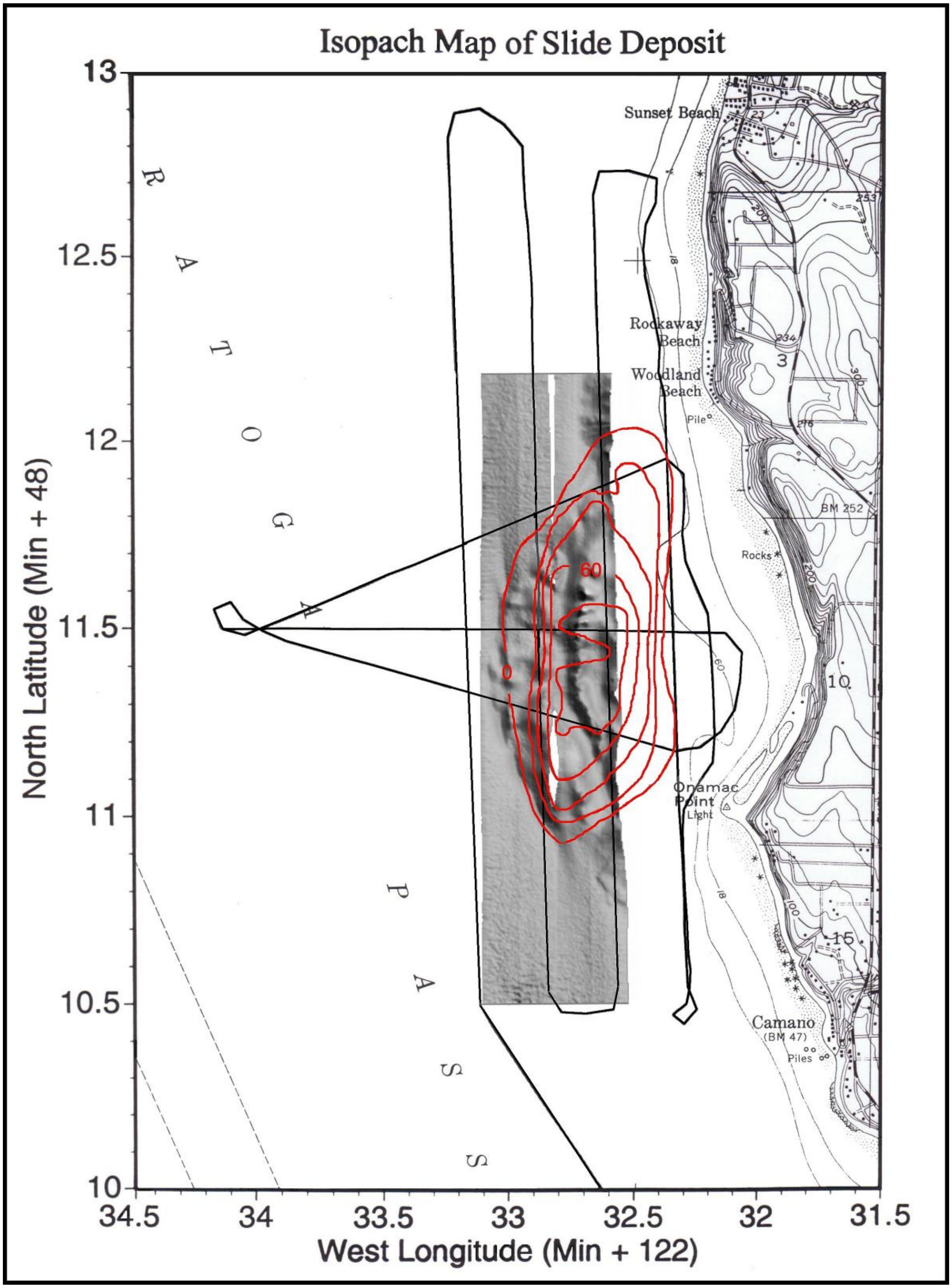
Isopach Map of Slide Deposit
North Latitude (Min + 48)
West Longitude (Min + 122)
13
12.5
12
11.5
11
10.5
10
34.5
34
33.5
33
32.5
32
31.5
Sunset Beach
Rockaway Beach
Woodland Beach
Pile
Rocks
BM 252
Onamac Point
Light
Camano
(BM 47)
Piles
60
0
S A R A T O G A P A S S

Figure 10

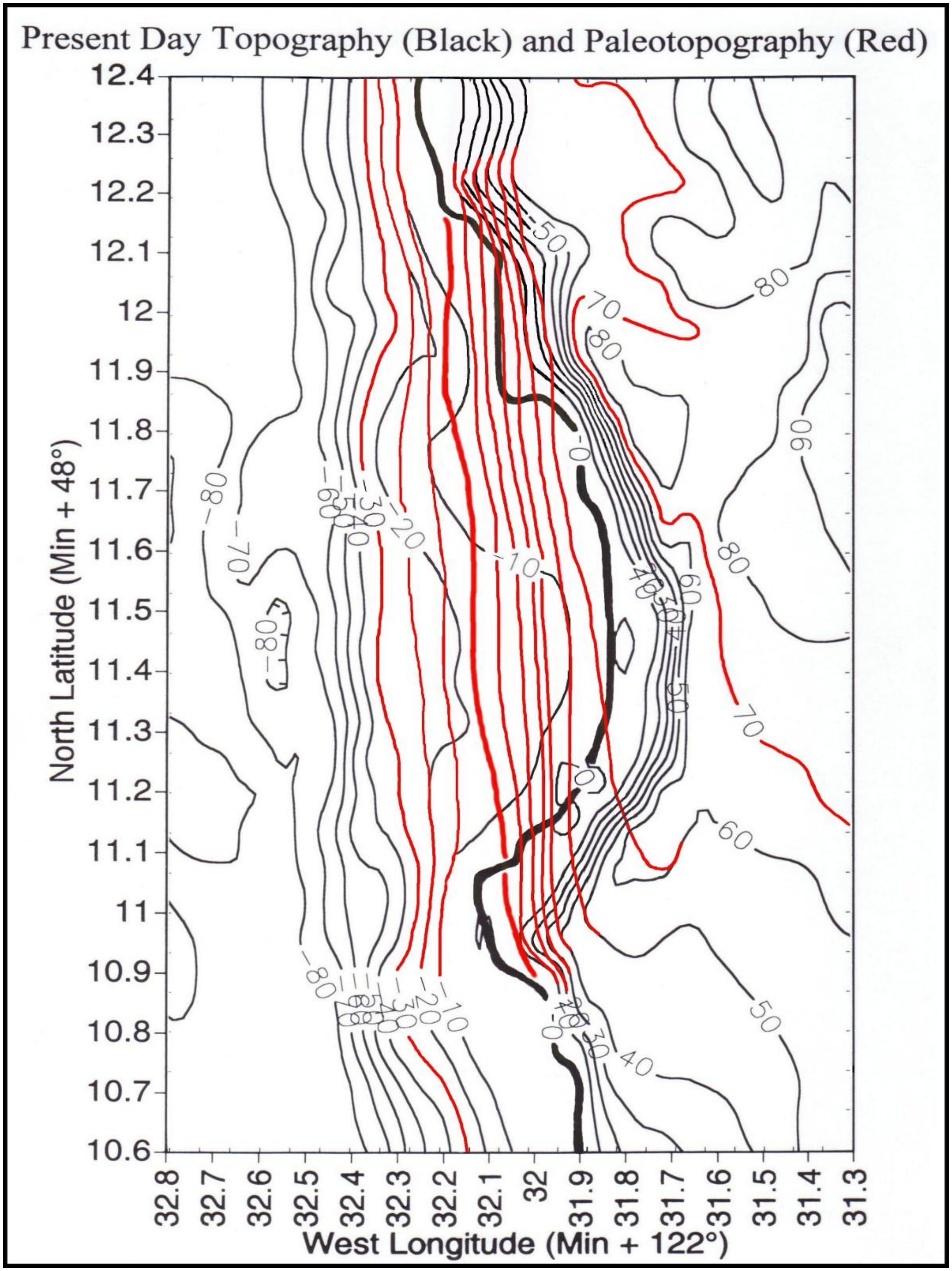

Present Day Topography (Black) and Paleotopography (Red)
North Latitude (Min + 48°)
12.4
12.3
12.2
12.1
12
11.9
11.8
11.7
11.6
11.5
11.4
11.3
11.2
11.1
11
10.9
10.8
10.7
10.6
32.8
32.7
32.6
32.5
32.4
32.3
32.2
32.1
32
31.9
31.8
31.7
31.6
31.5
31.4
31.3
West Longitude (Min + 122°)

Figure 11

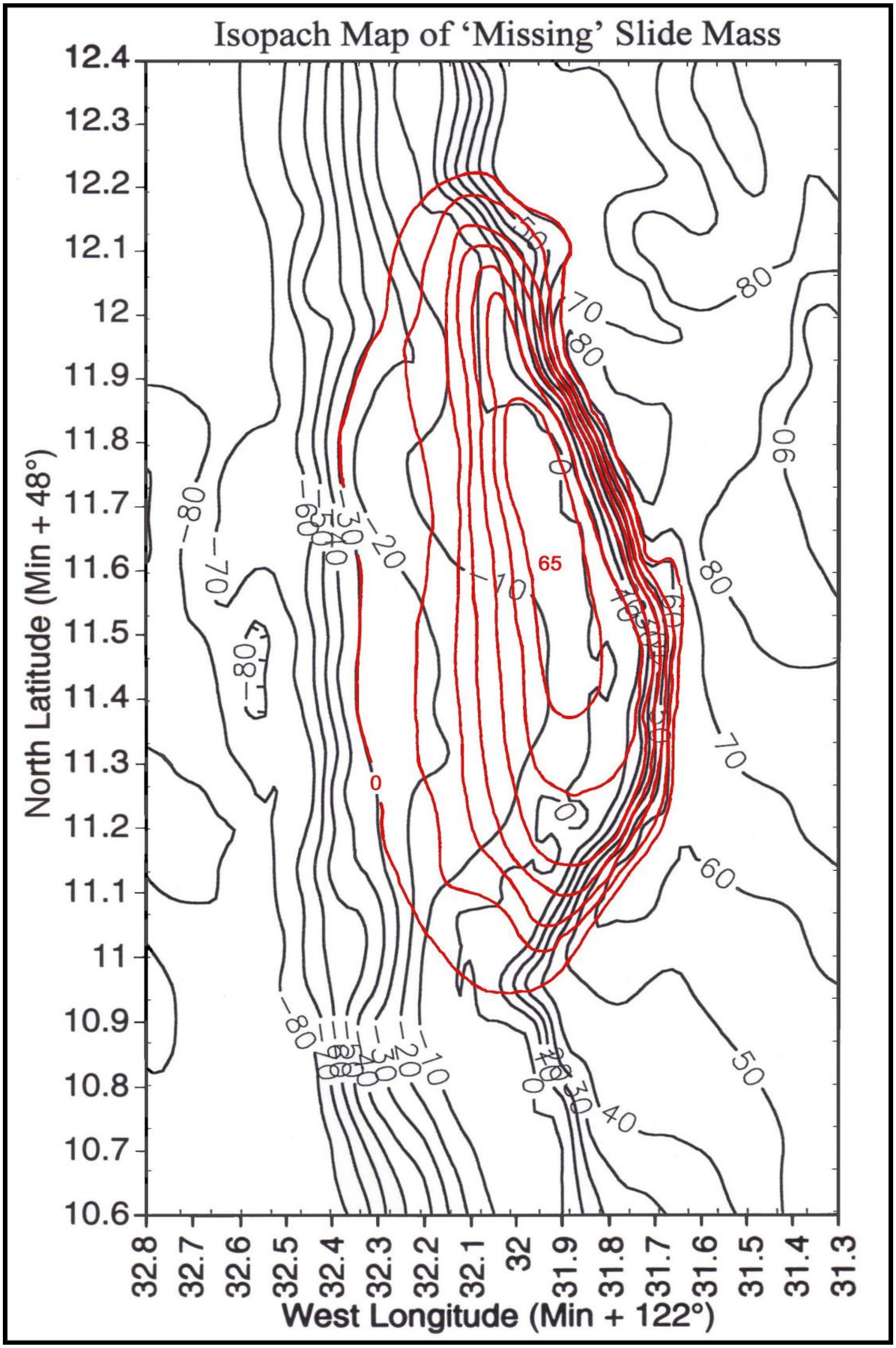
Isopach Map of 'Missing' Slide Mass
North Latitude (Min + 48°)
West Longitude (Min + 122°)
12.4
12.3
12.2
12.1
12
11.9
11.8
11.7
11.6
11.5
11.4
11.3
11.2
11.1
11
10.9
10.8
10.7
10.6
32.8
32.7
32.6
32.5
32.4
32.3
32.2
32.1
32
31.9
31.8
31.7
31.6
31.5
31.4
31.3
65
0